High-frequency, high-intensity electromagnetic field effects on Saccharomyces cerevisiae conversion yields and growth rates in a reverberant environment

Emmanuel Bertrand, Christophe Pasquier, David Duchez, Sebastien Girard, Agnès Pons, Pierre Bonnet, Catherine Creuly, Claude-Gilles Dussap

High-frequency, high-intensity electromagnetic field effects on *Saccharomyces cerevisiae* conversion yields and growth rates in a reverberant environment

Emmanuel Bertrand[a,b,d*], Christophe Pasquier[a,c], David Duchez[a,b], Sebastien Girard[a,c], Agnès Pons[a,b], Pierre Bonnet[a,c], Catherine Creuly[a,b] and Claude-Gilles Dussap[a,b]

[a] Université Clermont Auvergne, CS 60032, 63001 Clermont-Ferrand, France

[b] Institut Pascal, UMR CNRS 6602 Team GePEB, Chemical Engineering, Applied thermodynamics and Biosystems – BP 10448 F-63000 Clermont-Ferrand, France

[c] Institut Pascal, UMR CNRS 6602 Team PHOTON, Photonics, Waves, Nanomaterials – BP 10448 F-63000 Clermont-Ferrand, France

[d]Aix-Marseille Université, INRA, Polytech' Marseille, UMR 1163 Biodiversité et Biotechnologie Fongiques, 163 Avenue de Luminy, CP225, 13288 Marseille Cedex 09, France

*Corresponding author: Tel: +33 (0) 491 828 568;

Permanent address: emmanuel.bertrand@univ-amu.fr (E. Bertrand)

Abstract

Studies of the effects of electromagnetic waves on *Saccharomyces cerevisiae* emphasize the need to develop instrumented experimental systems ensuring a characterization of the exposition level to enable unambiguous assessment of their potential effects on living organisms. A bioreactor constituted with two separate compartments has been designed. The main element (75 % of total volume) supporting all measurement and control systems (temperature, pH, agitation, and aeration) is placed outside the exposure room whereas the secondary element is exposed to irradiation. Measurements of the medium dielectric properties allow the determination of the electromagnetic field at any point inside the irradiated part of the reactor and are consistent with numerical simulations. In these conditions, the growth rate of *Saccharomyces cerevisiae* and the ethanol yield in aerobic conditions are not significantly modified when submitted to an electromagnetic field of 900 and 2400 MHz with an average exposition of 6.11 $V.m^{-1}$ and 3.44 $V.m^{-1}$ respectively.

Highlights:

- Rational method to assess the intensity and specific absorption rate in submerged cultures developed
- The average mean electric field in submerged culture is respectively 6.11 and 3.44 $V.m^{-1}$ and the maximum local SAR is respectively 0.040 and 0.080 $W.kg^{-1}$ at 900 and 2400 MHz
- Liquid culture medium dielectric properties significantly limit the yeast exposition to the electromagnetic field
- No effect on growth rate and ethanol yield noticed

- Possible effect on glycerol and acetate yields to be further investigated

Keywords: Metabolic sensitivity to electromagnetic field; dielectric properties; *Saccharomyces cerevisiae*; ethanol production; mode-stirred reverberation chamber (MSRC).

1. Introduction

Electromagnetic stimulations are potentially effective to elicit either positive or adverse effects in many biological systems (Pilla and Markov, 1994). Given the diversity of exposition devices, frequencies, intensities, and durations used, the observed results appear sometimes contradictory (Hristov and Perez, 2011). In modern societies, the negative influence of intensive electromagnetic environment is one of the main concerns of the citizens in terms of public health. The French National Agency for Food, Environmental and Occupational Health and Safety (ANSES) stresses the need for better characterized experimental devices to ensure the accurate determination of the level of exposure to the electromagnetic fields to ensure an unequivocal assessment of their potential effects on living cells (ANSES, 2013). In any case, there is a considerable interest to improve a thorough understanding of the effects of electromagnetic radiation on living cells.

It is noteworthy that biofuels are a credible alternative for a more sustainable future with an important growth potential: in 2012 more than 93% of the 2500 millions of tons of oil equivalent used for transportation came from non-renewable feedstock (IEA, 2012) letting plenty of scope for improvements. It is also admitted that biomass production processes are requiring major improvements to make them economically competitive with their fossil equivalents (Menten, 2013; Chovau et al., 2013). Whatever the generation of bioethanol, *Saccharomyces cerevisiae* is the microorganism of choice to carry out alcoholic fermentation of sugars and has received considerable attention (Bertrand et al., 2016). In terms of process intensification, two complementary approaches are traditionally applied (Reay, 2008). Metabolic engineering and molecular biology, aims at amplifying the metabolic fluxes leading to an overexpression of the

interesting metabolites or at gaining functionalities such as the consumption of a new carbon source, for instance xylose to produce ethanol (Kim et al., 2013; Van Vleet and Jeffries, 2009), while process engineering aims at preventing mass transfer limitations (Hristov, 2010). Hunt et al. (2009) provide an extensive review of the use of electromagnetic fields for biofuels and bioenergy applications and the underlying possible mechanisms. In this context, the effects of electromagnetic fields in the ultra-high-frequency range (within the 300 MHz to 3 GHz bandwidth) have been few studied and quantified, although permanent magnets (da Motta et al., 2008; Muniz et al., 2007), predominant electric field at low frequencies (Perez et al., 2007), pulsed electric fields (Mattar et al., 2015) and sonication (Sulaiman et al., 2011; Indra Neel et al., 2012) have proven their potential for improving metabolites production. The mechanisms are not fully understood but some general trends are underlined depending on the electromagnetic frequency applied. Permanent magnets (i.e. static magnetic fields) have a major effect on the phospholipids orientation in the cell membrane affecting its biomechanical properties (Wang et al., 2014). They also help to preserve enzymes conformation and counterbalance the negative side effect of high ethanol concentration that alters cellular membranes and unfolds cytosolic globular enzymes (Lopes and Sola-Penna, 2001). Electric fields at low frequencies enable ionic redistribution as well as a higher potential difference in the cellular suspension. The effects of pulsed electric fields stimulations are largely unknown. It is hypothesized that a specific yeast subpopulation is favored knowing that cytoplasmic membrane modifications are induced by temporary electroporation (Mattar et al, 2015). External electric fields improve nutrient transportation through the modified cell membrane via pore formation or even transport proteins activations (Castro et al., 2012). An improved gas-liquid mass

transfer for dissolved carbon dioxide removal, which is known to inhibit *Saccharomyces cerevisiae* growth, is the main effect of Mild sonication on the culture broth leading to higher ethanol productivity (Indra Neel et al., 2012).

Therefore, depending on their settings, electromagnetic stimulations have potential to promote one or the other approaches for process intensification of *Saccharomyces cerevisiae* fermentation. In the high-frequency range, previous studies showed that high-frequency electromagnetic waves promote and stabilize free radicals in yeasts associated with oxidative stress. This effect is amplified when the intensity of the field increases (Crouzier et al., 2009). Oxidative stress can alter significantly the synthesis of reduced metabolites via redox mechanisms. The regulation of NADH homeostasis directly impacts redox balance and the metabolic fluxes distribution. According to Hou et al. (2010), an increase in mitochondrial NADH promotes ethanol production by restricting the entry of carbon into the TCA cycle while an increase in cytosolic NADH leads to glycerol production. However, these findings have not yet been investigated for bioethanol production improvements.

The two aims of this study are: (i) to develop and characterize a fully controlled and instrumented bioreactor for the culture of cells in a liquid medium under controlled electromagnetic stimulations; enabling both an off-line determination of metabolites concentrations and online assessment of growth rates by gas-phase analysis and mass balances. (ii) to master an intense oxidative stress on *Saccharomyces cerevisiae* cultures using high-frequency, high-intensity electromagnetic field to potentially trigger an overproduction of ethanol.

1. Materials and Methods

1.1. Exposition to the electromagnetic field

1.1.1. Dielectric measurements

For assessing the influence of electromagnetic stimulations one key variable is the electric properties of the culture medium. This is obtained measuring the complex permittivity (complex number).

The culture medium relative permittivity (ε_r) and electric conductivity (σ [$S.m^{-1}$]) were measured using a “Di-line” Transverse Electromagnetic sensor (INDEXSAR, Newdigate, United-Kingdom) at 30°C, the temperature set-point used for the culture. A vector network analyzer (Rohde & Schwarz ZVB8) was used to measure the transmission loss and phase of the TEM-line with or without the culture medium making it possible to compute the dielectric properties for all the frequencies used. Detailed explanations about the computation can be found in (Toropainen et al., 2000).

1.1.2. Mode Stirred Reverberation Chamber (MSRC)

To obtain a defined and controlled electromagnetic field, irradiated cultures have been performed in a specific chamber. The MSRC is a special device to obtain reproducible electromagnetic field generation (Fig. 1). A double-layered steel Faraday cage protects the experiment from external or environmental electromagnetic field. An antenna (ETS Lindgren 3144) is used to generate the electromagnetic field, while the walls and a stirrer reverberated randomly the incident waves within the cavity. Within a specific volume of the chamber, called working area (delimited by the blue points in Fig. 1), the electromagnetic field is statistically (i.e. for a full rotation of the stirrer) homogeneous and isotropic (Hill, 1994). The method is fully normative (IEC, 61000-4-21) and more explanations concerning the Institut Pascal’s MSRC properties and performances for the exposition of biological samples are available in (Lalléchère et al., 2010). The intensity of the electromagnetic field impacting the bioreactor is measured using an isotropic electric field antenna (PMM-EP 183).

1.1.3. Numerical Simulations

The main issue is to determine the accurate exposure field of the biomass submerged in the culture medium. A commercial software based on the method of moments (FEKO EM Software version 5.5, FEKO EM Software & Systems GmbH, Böblingen, Germany) coupled with an analytic approach was used to estimate the electromagnetic field impacting the culture compartment located inside the MSRC. For all the simulations performed with FEKO, the unstructured mesh has been sized so that the characteristic length is at least smaller than λ/4 at a frequency of 2400 MHz (the highest frequency used in this study is fixing the finer mesh that is necessary). However, due to calculation capacity limitations, numerical simulations of the reactor inside the MSRC at scale 1 were not possible. To overcome this limitation, we used MATLAB R2017a and obtained, from the theory of electromagnetic waves propagating inside a cavity the analytical expressions of the electromagnetic field at any point inside the MSRC, for each resonance mode of the chamber and for each propagation direction. The vectorial sum of these fields was then calculated to obtain the distribution of the total field in the MSRC for each Mode. As an example, Figure 2A represents the electric Field repartition for mode 7/33/14 at 900 MHz. As the MSRC has losses, there is no Dirac signal associated for a given Mode. It is observed a reduction in the signal amplitude spreading around the reference frequency that can be easily approximated by a Lorentzian (Fig. 2B) with the quality factor of the MSRC that has been previously determined for each frequency. At 900 MHz (Fig. 2C) and at 2400 MHz (Fig. 2D), several resonance modes are present in the MSRC. To accurately characterize the electromagnetic field, it is necessary to consider the contribution of each of these different Modes, which were also excited by the source at 900 or 2400 MHz. However, their impact must also be weighed against their frequency distance from the reference

frequency. The number of modes has been limited to those that are less than 5 times out of the Lorentzian bandwidth that is centered on the emission frequency of the source. The circles indicate the weighting coefficient used for the field strength of each mode considered. Once these modes have been determined, it is then possible to calculate the total Electric Field resulting from the vector sum of all these contributions and to obtain an evolutionary image of the amplitude of the E-field at the reactor site in the MSCR at 900 MHz (Fig 2E) and 2400 MHz (Fig 2F). The total computed electric field is compared with the well-known MSCR characteristics at 900 MHz and 2400 MHz to recalibrate the simulation results with the experimental conditions.

1.2. Cultures

Saccharomyces cerevisiae ATCC 7754 was kept at 4°C on an agar plate containing 3g yeast extract, 3g malt extract, 5g peptone and 10 g glucose per liter. A single colony is sub-cultured on a fresh plate and incubated for 48h at 30°C.

Culture media, 1 M NaOH solution (used for pH adjustment during the culture) and Antifoam A (Sigma-Aldrich, Illkirch, France) were sterilized for 20 min at 121°C. The inoculum was prepared by aseptically transplanting the yeast into a 500 mL Erlenmeyer flask containing 200 mL of the culture medium. It was formulated according to Kristiansen (1994) prescriptions to bring the strict necessary elements for the yeast's growth (Glucose: 50 $g \cdot L^{-1}$; KH_2PO_4 : 3$g \cdot L^{-1}$, $(NH_4)^2SO_4$: 2 $g \cdot L^{-1}$; vitamins, salts and minerals). The suspensions are then placed overnight at 30 °C under continuous shaking (200 rpm). Glucose concentrations were set to 10 and 50 $g \cdot L^{-1}$ for the inoculum and bioreactor cultures respectively.

The culture was operated on a 500 mL working volume instrumented Multifors bioreactor (Infors HT, Bottmingen, Swiss). The reactor is equipped with a pH probe, a

188 temperature controller, a sensor detecting the level of foam and a sensor measuring the
189 partial pressure of dissolved oxygen (pO2). The process was regulated at 30°C, 600 rpm
190 and pH 5.5. The bioreactor was connected to a secondary reactor (placed in the MSRC
191 for the electromagnetic field stimulations) consisting in a glass column (internal
192 diameter 5 cm, length 25 cm for a total volume of 490 mL) through 2* 10 m of flexible
193 tubes (internal diameter 0.8 mm). A Masterflex (ref 7518-10) peristaltic pump (Cole
194 Palmer, Vernon Hills, IL) let the medium circulates within the whole system at a flow
195 rate of 288 $mL \cdot min^{-1}$. A Luxtron SFT infrared pyrometer (LumaSense Technologies,
196 Santa Clara, CA) was used to assess the temperature of the secondary reactor during the
197 whole culture. Samples were taken out periodically and biochemical analyses were
198 carried out in duplicates.

199 1.3. Liquid phase analyses
200 Samples from the reactor were immediately filtered (on 0.2 µm hydrophilic filter) to
201 separate the medium from the biomass.

202 The dry cell weight was determined by measuring the optical density at 600 nm of a
203 yeast suspension with a spectrophotometer (BIOMATE 3S, ThermoFischer Scientific,
204 Illkirch, France) and correlated with 5 mL filtered and dried biomass (24 hours at 105
205 °C) weightings.

206 The filtrate was then deproteinized by the addition of 125 µL of barium hydroxide and
207 125 µL of zinc sulfate (5% w/v) and centrifuged at 10 000g for 5 minutes. The
208 supernatant was kept for the following analyses.

209 Organic acids, alcohols, and glucose were quantitated by HPLC. The separation is
210 carried out at 50°C in isocratic mode at an eluting flow rate of 0.7 $mL \cdot min^{-1}$ of a 5 mM

sulfuric acid solution on two Phenomenex Rezex ROA (7.8 × 300 mm) columns connected in series (Phenomenex, Le Pecq, France). Detection is performed by refractometry while the acquisition and the integration of chromatographic peaks rely on the HPChem (ver. A.08.03) software (Agilent, Massy, France). Quantitation is performed against a standard for the different compounds of interest. The detection limits of the various products are between 1 mg and 0.1 $g \cdot L^{-1}$.

Amino acids and ammonium ions were spectrocolorimetrically assayed according to a modified ninhydrin (Moore & Stein, 1948) or phenol-hypochlorite (Weatherburn, 1967) method respectively. Reactants were obtained from Sigma-Aldrich (St. Louis, MO, USA) and were of analytical grade (purity > 99.5%).

The exponential growth rates are determined by regression analysis (linear estimation) of biomass dry mass versus time in log scale. The production yields are determined by plotting the total quantity of products formed as functions of the total quantity of substrate consumed. The yields are determined by linear regression. The Monod hypothesis, which assumes constant yields, is verified in the case of the substrate concentration being tested. Standard deviations, variances and confidence intervals of the identified parameters (maximum growth rates and reaction yields) were calculated considering the most acceptable criterion is the mean square estimate.

In order to ensure the consistency of the various analyses carried out during the culture, the conservation balances of carbon (B_C) and nitrogen (B_N) were calculated assuming the following C molar formula for *Saccharomyces cerevisiae:* $CH_{1.6}O_{0.52}N_{0.15.}$

1.4. Gas phase analysis

The gas fraction was preliminarily dried in a drierite gas-drying unit (W. A. Hammond Drierite Co, Xenia, Ohio) and the molar fraction of oxygen and carbon dioxide were measured at the exhaust of the reactor using a ZRE gas analyzer (Fuji Electric, Clermont-Ferrand, France). Gaseous balances on the reactor lead to the instantaneous respiration rates according to the following equations:

G^e is the air molar flow rate feeding the reactor expressed in mmole·h^{-1}. V_r is the volume of the culture medium in the reactor at a specific time t. It is the initial volume of culture medium corrected with the volume of the different samples taken out during the culture and with the volume of the sodium hydroxide solution that has been added to the vessel to keep the desired pH. and are the specific oxygen consumption and carbon dioxide production rates expressed in mmol·L^{-1}·h^{-1}. is the molar oxygen fraction in the air feed (≈0.2093), while and are the molar fraction of oxygen and carbon dioxide in the dried air leaving the reactor.

The amounts of consumed oxygen and produced carbon dioxide expressed in mmol L^{-1} during the culture are calculated by integrating the instantaneous respiration rates according to the following equations:

For convenience, this integration was carried out digitally after discretization of a time interval Δt = 20s corresponding to the acquisition rate being set for the gas analyzer. The respiratory quotient RQ can then ultimately be calculated:

2. Results and Discussion

2.1. Exposition to the electromagnetic radiations

One of the fundamental issues is the selection of the most suitable exposure facility (Paffi et al., 2010). The actual electromagnetic environment is far more complex than a planar irradiation that is conventionally used for most of the bio-electromagnetism studies. In this context, the Mode Stirred reverberation chamber (MSRC) has proved to be an efficient tool for bioelectromagnetism stimulations (Lalléchère et al., 2010). Previous experiments carried out on vegetables such as *Lycopersicon esculentum* have proved the potential to induce transcription, translation and even ATP concentration changes at high-frequency and even low intensity such as 5 $V \cdot m^{-1}$ (Roux et al., 2007). However, this type of environment cannot accommodate with any type of electrical devices whose presence is likely to alter the ideal distribution of the electromagnetic field. Conversely, electronic cards may be damaged by an exposition to intense electromagnetic radiations. A reproducible microbial culture must necessarily be carried out in a regulated and controlled bioreactor. However, the presence of the entire system including all the regulation devices inside the exposure chamber was not an option as the electromagnetic field might damage the electronic parts of the system. Therefore, the instrumented bioreactor was coupled with a secondary exposition vessel to examine the biological effects of the electromagnetic field. The suspension was recycled through the MSRC as shown in Fig. 3. The connecting pump flow rate is 288 $mL \cdot min^{-1}$. Under these conditions, the residence time in the secondary element is 94s (0.45 L), which corresponds to an exposition to the electromagnetic waves for 25% of the culture time. In the other parts (including the main culture vessel and the connecting parts) the residence time was 280s (1.35 L).

2.2. Measurements of the medium dielectric properties

A frequency scanning from 600 to 2500 MHz (Fig. 3) indicates that the relative permittivity of the yeasts suspension (minimal medium) is slowly decreasing from 78 to 74 while the electric conductivity is sharply increasing from 0.4 to 2.5 $S \cdot m^{-1}$. These measurements agree with the behavior of an electrolyte solution such as saline water (Gadani et al., 2012). Additionally, to the frequency being applied, the initial composition of the culture medium is of importance. For instance, the addition of ammonium sulfate into the minimal medium, which aims at bringing nitrogen into available form, also brings sulfate as a counter ion. This has the side effect to considerably increase the medium conductivity. The measurements have shown that at any frequency the conductivity for the minimal medium is about 0.5 $S \cdot m^{-1}$ higher than the one for the yeast medium. The production of biomass and metabolites (ethanol, glycerol, acetate) during the culture are also susceptible to continuously modify the dielectric properties of the culture medium. At lower frequencies, in the kHz range near the β-relaxation zone, these properties are exploited to develop online biomass sensors (Martisen, Grimmes and Schwan, 2002). However, a preliminary study has shown that these changes in the high-frequency range (600 to 2500 MHz) have no significant effect on the medium conductivity but may lead to a 10% increase of the medium permittivity. The filtration of the medium for removing the biomass also indicates that these changes are related to the metabolites and not to the presence of the yeasts themselves in the medium (data not shown). Starting the fermentation with a 50 $g \cdot L^{-1}$ glucose concentration does not lead to any significant changes in the medium dielectric properties (Fig 3). Therefore, the exposition to the electromagnetic field could be considered identic throughout the culture. It is further noteworthy to mention that a higher conductivity leads to a higher attenuation of the electromagnetic waves inside the

medium. This had an impact on the reactor design. Its shape must be thin enough to permit a homogenous exposition of the yeasts to the electromagnetic field.

2.3. Numerical Simulations in an anechoic environment

Numerical simulations were used to assess the influence of the geometry, the material properties and of the thickness of the secondary reactor element and their impact on the electromagnetic waves propagation. Due to the complexity of the real electromagnetic environment, a straightforward approach was to consider the incident electromagnetic field as a plane wave. The assumption is thus to consider the culture is in an anechoic environment. Using FEKO electromagnetic simulation software, various reactors configurations were illuminated by a plane wave at the two frequencies selected for the study: 900 MHz and 2400 MHz. Results from these preliminary simulations indicate that the use of Pyrex glass or polyethylene does not induce any significant changes in the electromagnetic profile observed in the culture medium. The selected materials appeared globally transparent in the frequency range studied.

The simulation of electromagnetic field propagation at 900 MHz and 2400 MHz has different profiles for the same incident power. The maximum amplitude of the electric field penetrating inside the reactor is 3 times more intense in the case of the exposition at 900 MHz than with the exposition at 2400 MHz. This is both due to the electric conductivity increase in the medium, from 0.9 to 2.3 $S.m^{-1}$ (Fig 3.) and the frequency shift (skin effect). It can be noticed that the intensity of the field is truly heterogeneous in the anechoic configuration as it can be seen in the cross sections presented in figure 4A.

In order to validate these simulations results, a direct measurement of the electromagnetic field in the culture medium has been performed. The experimental

measurement of an electromagnetic field inside a liquid is in itself a challenge. In fact, as small as the probes may be, these latter are intrusive and not pointwise. Therefore, the measurement is the result of integration over a finite volume element. It is therefore not possible to access the measurement with a millimetric (or even centimetric) spatial resolution. This is even accentuated when the field intensity rapidly changes inside the measurement volume. Moreover, the probes are generally developed in order to perform field measurements in the air and not directly into liquids. Before being immersed in culture broth, the probe should be protected in a sealed glass tube, which then creates new interfaces and further possible electromagnetic reflections. Finally, the probe itself can interfere with the electromagnetic environment. In this case, it is likely that the electric field intensity measured by the probe is not that prevailing in its absence. Thus, the effect of the perturbation introduced by the probe on the electromagnetic environment must be investigated numerically.

Experimental measurements were performed in the empty reactor and after having it filled with the medium so that the position of the probe has not been modified. The results indicate that 68 % of the electric field amplitude measured in the empty reactor is effectively transmitted at the center of the culture medium. These experimental results are not in agreement with the numerical simulations that indicate that 18% of the incident field is effectively transmitted (Fig. 4B). This discrepancy has been explained by the impact of the insertion of the probe into the reactor, proving an experimental bias introduced by the probe. Four simulations have been performed successively. The first one concerns the empty reactor. The second simulation accounts for the effect of the liquid medium electromagnetic properties when the reactor is filled with the culture medium. The third simulation introduces a fictive glass cylinder filled with air,

simulating the tube protecting the measuring probe. The fourth simulation accounts for a small diameter conductive cylinder in to simulate the probe itself (Fig 4B). The simulation results show that the effect of the probe agrees with the measured values. This permits to validate the simulation results and confirm the calculation of the electric field that is transmitted to the cells in culture conditions, i.e. 18 %, whereas the experimental value is 68 % due to probe effects.

The simulation of the impact of the probe tends to strengthen the confidence in the field values determined numerically and indicates that the field experimental values obtained by the probe are not fully representative of the level that is actually perceived by the culture medium in the irradiated part due to the modification of the electromagnetic environment introduced by the probe itself. The recent commercialization of sub-millimeter electro-optical sensor, adapted to the field of measurement in liquid media and even plasma might be a valuable solution to improve the experimental mapping of field profiles in the irradiated part of the reactor (Jarrige et al., 2012).

2.4. Electromagnetic field propagation inside the yeast itself

Depending on the frequency, the propagation of the electromagnetic field inside the cells might schematically vary between two extreme schemes. Either the wave passes through the yeast cells without any attenuation, or for the lowest frequencies, the yeast will be shielded and therefore preventing any possible action of the electromagnetic field (Hristov and Perez, 2011). Advances in dielectrophoresis (Asami, 2002) associated with single cell impedance spectroscopy make it possible to extract with a relatively good accuracy both relative permittivity and medium electric conductivity at subcellular lever for frequencies from 0 up to 500 MHz (Haandbæk et al., 2014). Given technical limitations, there does not exist any data at subcellular scale for frequencies higher than

500 MHz. Therefore, these values must be considered the best estimations currently available. Based on these data, the propagation of the electromagnetic field waves has been simulated inside semi-infinite planes having the dielectric properties of the diverse cellular sub-compartments. The results indicate that the electromagnetic wave propagates very efficiently inside the cell wall, is only slightly attenuated by the cell membrane and is mostly attenuated by the cytoplasm of the cell. Given the size of the yeast, we have estimated that more than 99% of the electromagnetic field impacting the yeast passes effectively through. Another important fact is that the dielectric properties of the cytosolic compartment determined by Haandbæk et al. study, (2014) are close to that observed for the culture medium. Hence, it seems appropriate to approximate the specific absorption rate of a yeast suspension by that of the culture medium in the irradiated part of the reactor.

2.5. Numerical study in the reverberant environment

Since the reactor temperature is regulated, it is not possible to evaluate the specific absorption rate (SAR) by measuring the temperature rise of the culture medium. Besides, infrared monitoring of the temperature in the irradiated part of the reacting volume showed no significant variations during the illumination (compared to the control culture). To estimate the SAR and its maximum value, the electromagnetic field strength in the reverberant environment must be calculated according to the dielectric properties of the culture medium. For computation capabilities reasons it was not possible to simulate the Institute Pascal experimental MSRC (L = 8.4 m; l=6.7 m, H = 3.5 m) directly at the chosen frequencies. In order to determine the field cartography and to estimate the SAR, FEKO simulations in free space and an analytic approach were combined. First, using FEKO the reactor was illuminated with three different waves at

900 MHz and 2400 MHz in free space. These directions represent the three directions of the different modes present in the MSCR. The profiles of the simulated electric field at 900 MHz and 2400 MHz according to these three directions are presented in Fig. 5. From these results, it was possible to determine the maximum percentage of the electric field penetrating the reactor. According to the simulations, the maximum value of 95 % was obtained. This value has been taken as a reference to compute the electric field intensity inside the MSCR according to the analytic approach presented previously. Secondary knowing the percentage maximizing the effects inside the reactor, it was possible to calculate the local SAR (SAR without mass or volume) inside the reactor for 20 000 points chosen arbitrarily in the reactor volume. SAR and local SAR expression are given by the following equations:

The repartition of the different values of the 20 000 random positions in the reactor is given in Fig. 5E for 900 MHz and Fig. 5F for 2400 MHz. The mean field strength, the average local SAR and the maximum local SAR corresponding to the experimental conditions are given in Table 1.

Values obtained are far below the threshold of 2 $W.kg^{-1}$ that is normally used to distinguish non-thermal and thermal effects. It should also be noted that the yeast cells are also set into motion by the hydrodynamics of the system, which is also contributing to the exposure homogeneity although it was not possible to model this numerically.

2.6. *Saccharomyces cerevisiae* batch culture results

The control experiment was carried out by maintaining the recycling loop during the culture without any application of the electromagnetic field inside the MSRC. The same

procedure has been applied for irradiated experiments except for the switching-on of the device for generating electromagnetic waves. The results are reported and compared in table 1 and Figure 6. The yields and the maximum growth rate are calculated by linear regressions. The growth rates and ethanol yields reported in this study are typical for Crabtree positive yeasts operated under aerobic conditions. It leads simultaneously to high fermentation yields (0.4 g per g of substrate) and relatively low biomass yields (0.13g per g of substrate) as reported by Albergaria and Arneborg (2016).

Contrary to the results observed with permanent magnets or at low frequencies magnetic waves by Da Motta et al. or Perez et al. (2007), there is no evidence for an effect both on the maximum growth rate and on the main conversion yields between the main components (biomass, glucose, ethanol, O_2 and CO_2), considering the standard deviations of the identified parameters. This means that the specific rates remain identical in exposed and in reference non-illuminated conditions. Contrarily, the glycerol and acetate yields seem very slightly affected by irradiation, by a factor of 1.2-1.5. This may be related to a perturbed status of redox intracellular balance due to the electromagnetic field. However, the global carbon and nitrogen balances do not appear to be affected, given the accuracy of the measurements. As the various reactions yields, as well as the respiratory coefficient, do not indicate any significant change, it is considered that the global stoichiometry of growth and of the production of primary metabolites by *Saccharomyces cerevisiae* are not influenced by an exposure of 25% of the culture vessel to high-frequency high-intensity electromagnetic fields. These results are close to the reported results obtained by Anton-Leberre et al. (2010) who did not find any effect of high static or even pulsed magnetic fields on the cellular processes of the yeast *Saccharomyces cerevisiae*. Nevertheless, this study brings a rational estimation

of actual volume, intensity, specific absorption rate and distribution of electromagnetic fields inside the culture medium, confirming the observation given by Anton-Leberre et al. (2010) with strictly controlled and quantified electromagnetic field conditions.

2.7. Recommendation and perspectives for further studies for assessing the effects of electromagnetic fields in submerged cultures

The study on the effect of electromagnetism waves impacting a living organism requires a specific and adequately characterized experimental device. The development of such a system has been done. Three important remarks must be done: (i) the exposure time is limited in comparison with the total culture time (about 25% in the present study); (ii) the intensity of the electromagnetic field actually transmitted to the cells is significantly attenuated in comparison to that impacting the irradiated part of the reactor (30% at 900 MHz and less than 20% at 2400 MHz) in a anechoic environment; (iii) the direct experimental measurement of the intensity of the electromagnetic field into the fermenting medium is technically impossible due to the changes of the confined electromagnetic environment caused by the probe itself. Direct measurements provide over-estimated values of the electric field intensity, ignoring the shielding effect of the aqueous medium itself. This requires the systematic use of numerical simulations for assessing the actual field of radiation perceived by the cells. This also underlines the need for sensors (such as electro-optic probes) capable to function in a liquid medium without disrupting the overall electromagnetic environment. The use of an exposure chamber in its reverberation configuration is mandatory since it achieves an electromagnetic field strength that is substantially greater in the secondary reactor in comparison from its anechoic configuration. Moreover, it allows obtaining a much more uniform and homogeneous electromagnetic environment regarding the amplitude of the field. Because of culture medium recirculation, the hydrodynamics inside the reactor as

well as the sinusoidal properties of the electric field, it must be considered that cells have been statistically exposed in a much more homogeneous way, considering they are crossing randomly the different regions of the liquid phase.

In the characterized electromagnetic environment as described previously, it has been observed that no biological specific response on the biomass, glucose, ethanol, CO_2 and O_2 yields was macroscopically observed at frequencies of 900 and 2400 MHz, with an emitted intensity average intensity perceived by the cells of 6.1 $V \cdot m^{-1}$ and 3.44 $V \cdot m^{-1}$ respectively applied on 25 % of the reacting volume. This suggests that a high-frequency, electromagnetic field does not induce any major modification of the ethanol production rate by *Saccharomyces cerevisiae*. However, it is observed that the conversion yields to glycerol and acetate decreased by a factor of 1.2 – 1.5 compared to non-irradiated conditions. Further investigations would be needed to determine whether the absence of observed biological effect is associated with a protecting role of the liquid culture medium that behaves like a “high cut filter” thus significantly limiting the yeast exposition to the electromagnetic field or to the absence of actual interaction between the high-frequency electromagnetic fields with the metabolism of *Saccharomyces cerevisiae*. In this context, the increase of the emitted power with the use of a pulsed electromagnetic field, or the design of an exposure device associating an internal source for the electromagnetic waves emission in a waveguide with specific dimensions to select the pertinent wavelength could be an interesting option to investigate.

3. Conclusion

The present study develops a rationale method for assessing rigorously the intensity and the specific absorption rate (SAR) of electromagnetic waves in submerged cultures of

Saccharomyces cerevisiae. For the frequencies 900 MHz and 2400 MHz, the average mean electric field was respectively 6.11 and 3.44 $V.m^{-1}$ and the maximum local SAR was respectively 0.040 and 0.080 $W.kg^{-1}$ well below the onset of thermal effects. With irradiation of 25 % of the culture medium, no effect on growth rate and ethanol yield is noticed, though significant deviations are observed for glycerol and acetate yields, showing a possible secondary effect on redox metabolic balance that needs to be further investigated.

Acknowledgments

This work has been sponsored by the French government research program "Investissements d'Avenir" through the IMobS3 Laboratory of Excellence (ANR-10-LABX-16-01), by the European Union through the program Regional competitiveness and employment 2007-2013 (ERDF – Auvergne region), and by the Auvergne region.

References

1. ANSES, Rapport d'expertise collective. "Radiofréquences et santé ", n° 2011-SA-0150, October 2013
2. Anton-Leberre, V., Haanappel, E., Marsaud, N., Trouilh, L., Benbadis, L., Boucherie, H., Massou, S., François, J.M., 2010. Exposure to high static or pulsed magnetic fields does not affect cellular processes in the yeast *Saccharomyces cerevisiae*. Bioelectromagnetics 31, 28-38.
3. Albergaria, H., Arneborg, N., 2016. Dominance of *Saccharomyces cerevisiae* in alcoholic fermentation processes: role of physiological fitness and microbial interactions. Applied Microbiology and Biotechnology 100, 2035–2046.
4. Asami, K., 2002. Characterization of biological cells by dielectric spectroscopy. J.Non-Cryst. Solids 305, 268–277.
5. Bertrand, E., Vandenberghe, L.P.S., Soccol, C.R., Sigoillot, J.-C., Faulds, C., 2016. First Generation Bioethanol, in Soccol, C.R., Brar, S.K., Faulds, C., Ramos, L.P. (Eds.), Green Fuels Technology, Biofuels. Springer International Publishing, Cham, pp. 175–212.
6. Castro, I., Oliveira, C., Domingues, L., Teixeira, J.A., Vicente, A.A., 2012. The Effect of the Electric Field on Lag Phase, β-Galactosidase Production and Plasmid Stability of a Recombinant *Saccharomyces cerevisiae* Strain Growing on Lactose. Food Bioprocess Technol. 5, 3014–3020.
7. Chovau, S., Degrauwe, D., Van der Bruggen, B., 2013. Critical analysis of techno-economic estimates for the production cost of lignocellulosic bio-ethanol. Renew. Sustain. Energy Rev. 26, 307–321.
8. Crouzier, D., Perrin, A., Torres, G., Dabouis, V., Debouzy, J.-C., 2009. Pulsed electromagnetic field at 9.71GHz increase free radical production in yeast (*Saccharomyces cerevisiae*). Pathol. Biol. 57, 245–251.

9. Da Motta, M.A., Muniz, J.B.F., Schuler, A., da Motta, M., 2008. Static Magnetic Fields Enhancement of *Saccharomyces cerevisiae* Ethanolic Fermentation. Biotechnol. Prog. 20, 393–396.
10. Gadani, D.H., Rana, V.A., Bhatnagar, S.P., Prajapati, A.N., Vyas, A.D., 2012. Effects of salinity on the dielectric properties of water. Indian J. Pure Appl. Phys. 50, 405–410.
11. Haandbæk, N., Bürgel, S.C., Heer, F., Hierlemann, A., 2014. Characterization of subcellular morphology of single yeast cells using high frequency microfluidic impedance cytometer. Lab. Chip 14, 369
12. Hill, D.A., 1994. Electronic mode stirring for reverberation chambers. IEEE Trans. on Electromagn. Compat. 36, 294-299.
13. Hou, J., Scalcinati, G., Oldiges, M., Vemuri, G.N., 2010. Metabolic Impact of Increased NADH Availability in *Saccharomyces cerevisiae*. Appl. Environ. Microbiol. 76, 851–859.
14. Hristov, J., 2010. Magnetic field assisted fluidization – a unified approach. Part 8. Mass transfer: magnetically assisted bioprocesses. Rev. Chem. Eng. 26.
15. Hristov, J., Perez, V.H., 2011. Critical analysis of data concerning *Saccharomyces cerevisiae* free-cell proliferations and fermentations assisted by magnetic and electromagnetic fields. Int. Rev. Chem. Eng. 3, 3–20.
16. Hunt, R.W., Zavalin, A., Bhatnagar, A., Chinnasamy, S., Das, K.C., 2009. Electromagnetic Biostimulation of Living Cultures for Biotechnology, Biofuel and Bioenergy Applications. Int. J. Mol. Sci. 10, 4515–4558.
17. IEA, 2012. World Energy Outlook 2012. OECD Publishing.
18. Indra Neel, P., Gedanken, A., Schwarz, R., Sendersky, E., 2012. Mild Sonication Accelerates Ethanol Production by Yeast Fermentation. Energy Fuels 26, 2352–2356.
19. Jarrige, P., Gaborit, G., Duvillaret, L., Kohler, S., Ticaud, N., Arnaud-Cormos, D., Lévèque, P., 2012. Electro-Optic Probe Devoted to Simultaneous Electric-Field and

555 Temperature Measurements in Biological Media for Dosimetric Assessments. Radio Sci.
556 Bull. 342, 5–15.
557 20. Kim, S.R., Park, Y.-C., Jin, Y.-S., Seo, J.-H., 2013. Strain engineering of *Saccharomyces*
558 *cerevisiae* for enhanced xylose metabolism. Biotechnol. Adv. 31, 851–861.
559 21. Kristiansen, B., & European Federation of Biotechnology. (1994). *Integrated design of a*
560 *fermentation plant: The production of baker's yeast*. Weinheim: VCH.

561 22. Lalléchère, S., Girard, S., Roux, D., Bonnet, P., Paladian, F., Vian, A., 2010. Mode stirred
562 reverberation chamber (MSRC) : A large and efficient tool to lead high frequency
563 bioelectromagnetic in vitro experimentation. Prog. Electromagn. Res. B 26, 257–290.
564 23. Lopes, D.H.J., Sola-Penna, M., 2001. Urea Increases Tolerance of Yeast Inorganic
565 Pyrophosphatase Activity to Ethanol: The Other Side of Urea Interaction with Proteins.
566 Arch. Biochem. Biophys. 394, 61–66.
567 24. Martinsen, O.G. Grimmes, S. and Schwan, H.P., 2002. “Interface Phenomena and
568 Dielectric Properties of Biological Tissues.” In *Encyclopedia of Surface and Colloïd*
569 *science*, 2643-2652, Marcel Dekker Ed.

570 25. Mattar, J.R., Turk, M.F., Nonus, M., Lebovka, N.I., El Zakhem, H., Vorobiev, E., 2015. *S.*
571 *cerevisiae* fermentation activity after moderate pulsed electric field pre-treatments.
572 Bioelectrochemistry 103, 92–97.
573 26. Menten, F., Chèze, B., Patouillard, L., Bouvart, F., 2013. A review of LCA greenhouse gas
574 emissions results for advanced biofuels: The use of meta-regression analysis. Renew.
575 Sustain. Energy Rev. 26, 108–134.
576 27. Muniz, J.B., Marcelino, M., Motta, M. da, Schuler, A., Motta, M.A. da, 2007. Influence of
577 static magnetic fields on S. cerevisiae biomass growth. Braz. Arch. Biol. Technol. 50,
578 515–520.

28. Paffi, A., Apollonio, F., Lovisolo, G.A., Marino, C., Pinto, R., Repacholi, M., Liberti, M., 2010. Considerations for Developing an RF Exposure System: A Review for in vitro Biological Experiments. IEEE Trans. Microw. Theory Tech. 58, 2702–2714.
29. Pilla, A.A., Markov, M.S., 1994. Bioeffects of weak electromagnetic fields. Rev. Environ. Health 10, 155–169.
30. Perez, V.H., Reyes, A.H., Justo, O.R., Alvarez, D.C., Alegre, R.M., 2007. Bioreactor Coupled with Electromagnetic Field Generator: Effects of Extremely Low Frequency Electromagnetic Fields on Ethanol Production by *Saccharomyces cerevisiae*. Biotechnol. Prog. 23, 1091-1094
31. Reay, D., 2008. The role of process intensification in cutting greenhouse gas emissions. Appl. Therm. Eng. 28, 2011–2019.
32. Roux, D., Vian, A., Girard, S., Bonnet, P., Paladian, F., Davies, E., Ledoigt, G., 2007. High frequency (900 MHz) low amplitude (5 $V \cdot m^{-1}$) electromagnetic field: a genuine environmental stimulus that affects transcription, translation, calcium and energy charge in tomato. Planta 227, 883–891.
33. Sulaiman, A.Z., Ajit, A., Yunus, R.M., Chisti, Y., 2011. Ultrasound-assisted fermentation enhances bioethanol productivity. Biochem. Eng. J. 54, 141–150.
34. Toropainen, A., Vainikainen, P., Drossos, A., 2000. Method for accurate measurement of complex permittivity of tissue equivalent liquids. Electron. Lett. 36, 32.
35. United Nations, 2013. World Population Prospects: The 2012 Revision., Department of Economic and Social Affairs, Population Division.
36. Van Vleet, J., Jeffries, T., 2009. Yeast metabolic engineering for hemicellulosic ethanol production. Curr. Opin. Biotechnol. 20, 300–306.

602 37. Wang, Z., Hao, F., Ding, C., Yang, Z., Shang, P., 2014. Effects of static magnetic field on
603 cell biomechanical property and membrane ultrastructure: Cell Mechanical Property in
604 SMF. Bioelectromagnetics 35, 251–261.
605 38. Weatherburn, M.W., 1967. Phenol-hypochlorite reaction for determination of ammonia.
606 Anal. Chem. 39, 971–974.

607 **Figures**

608 **Fig. 1:**

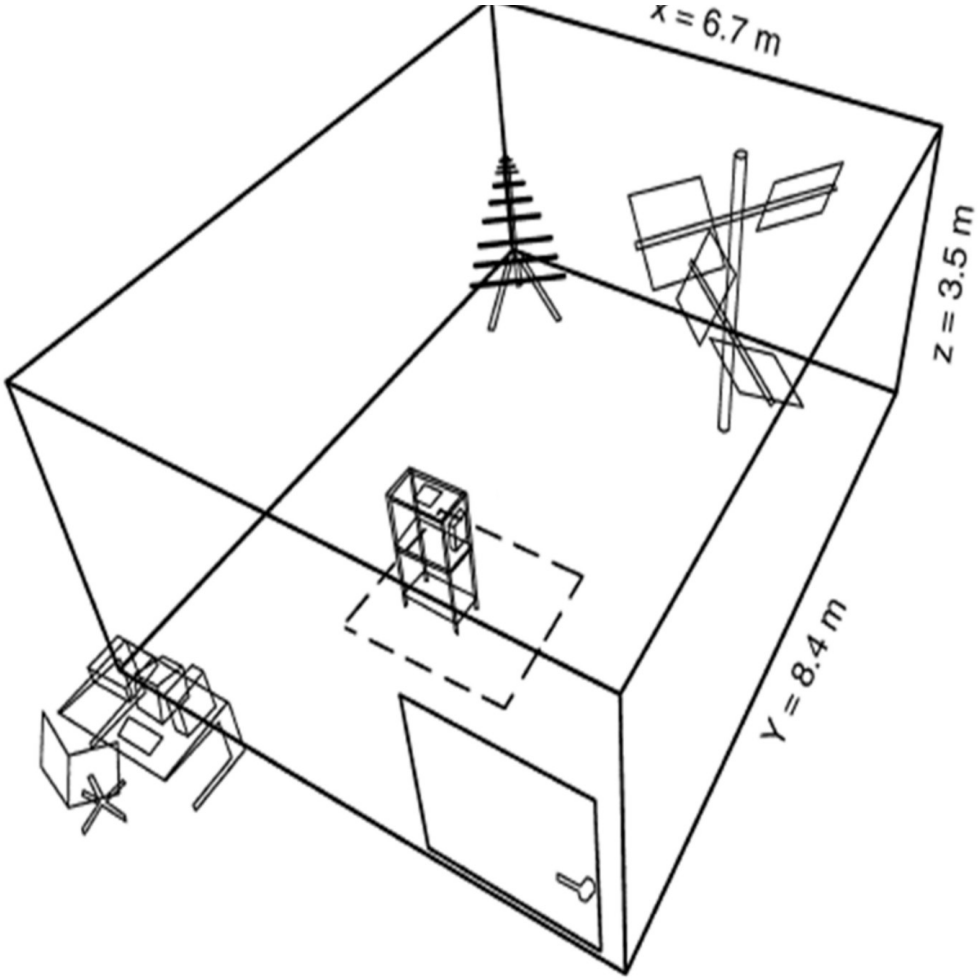

609

610 **Fig. 2:**

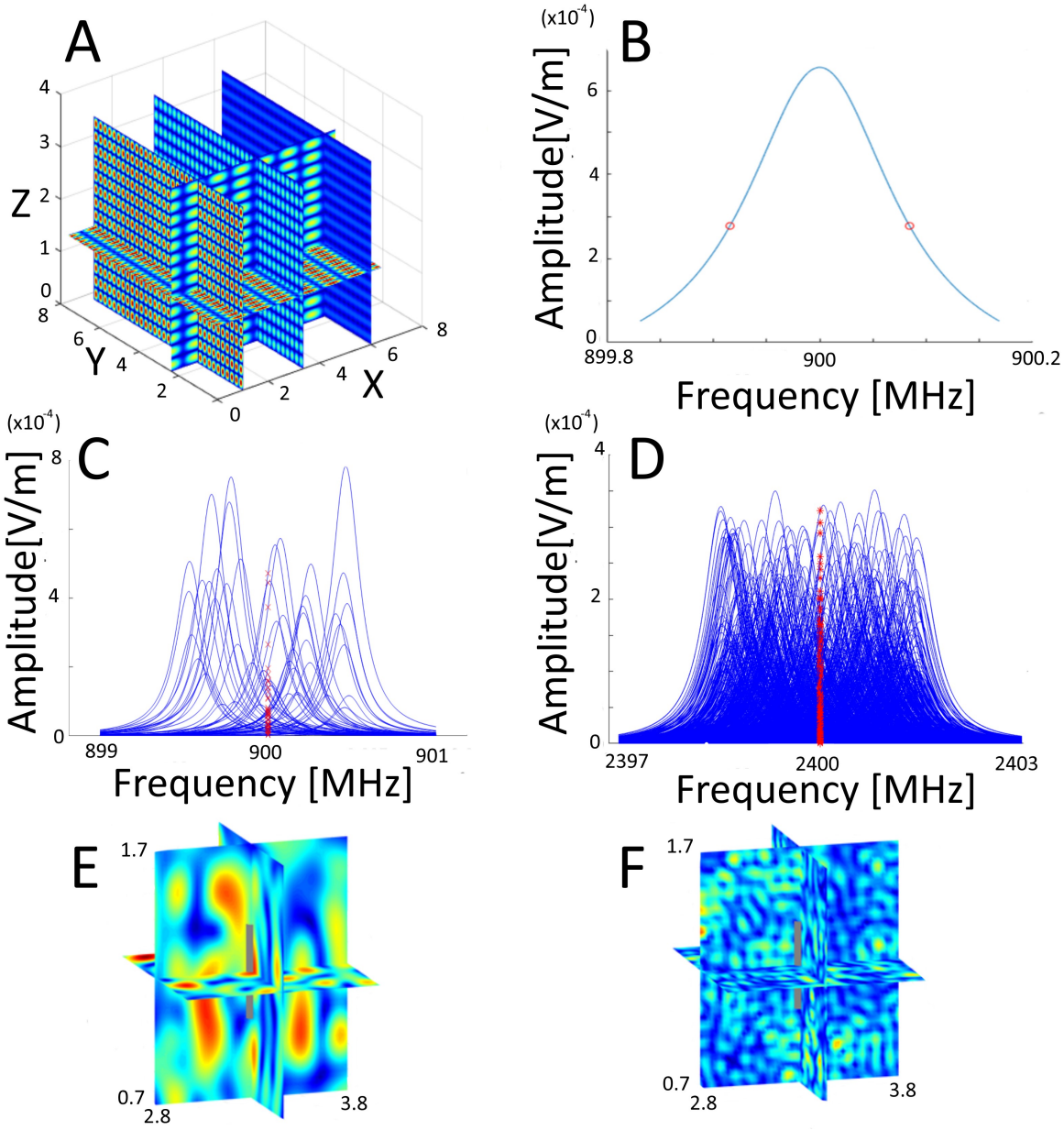

611

612

613 **Fig. 3:**

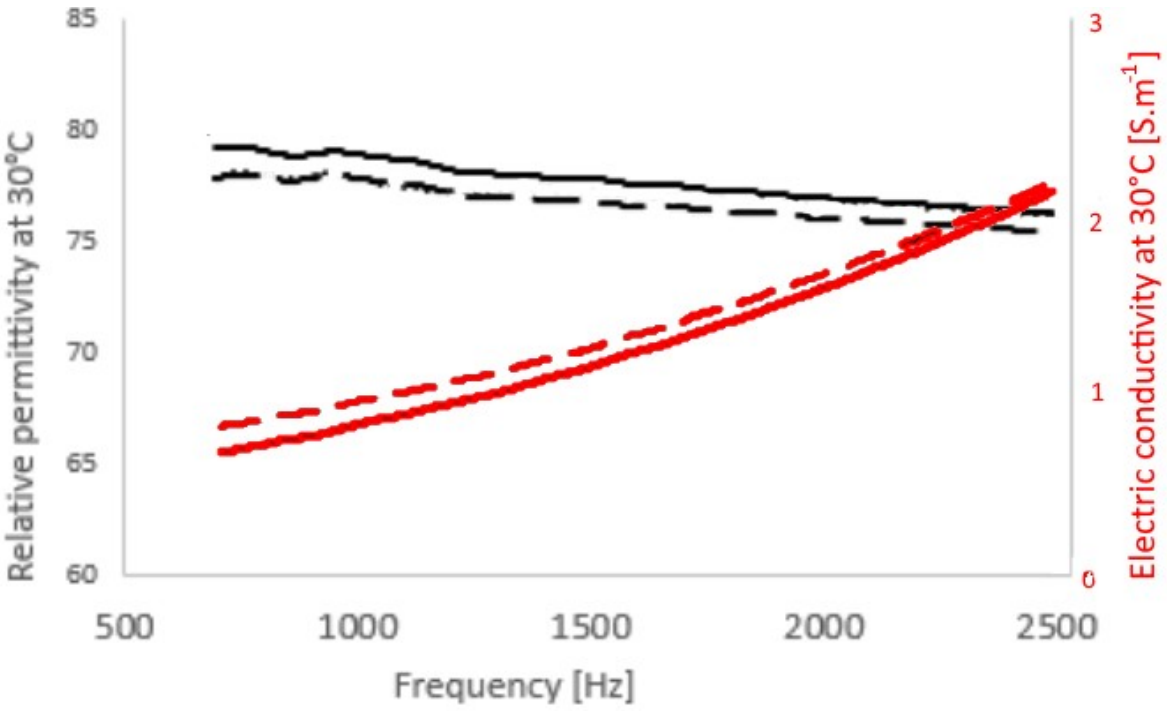

614

615 **Fig. 4:**

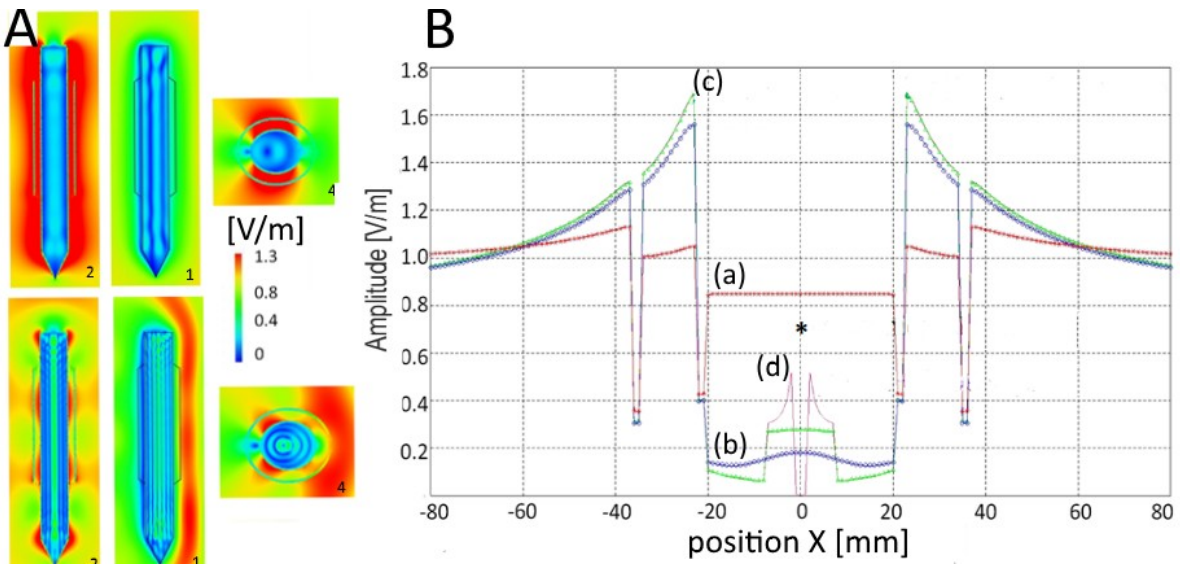

616

617

618 **Fig. 5:**

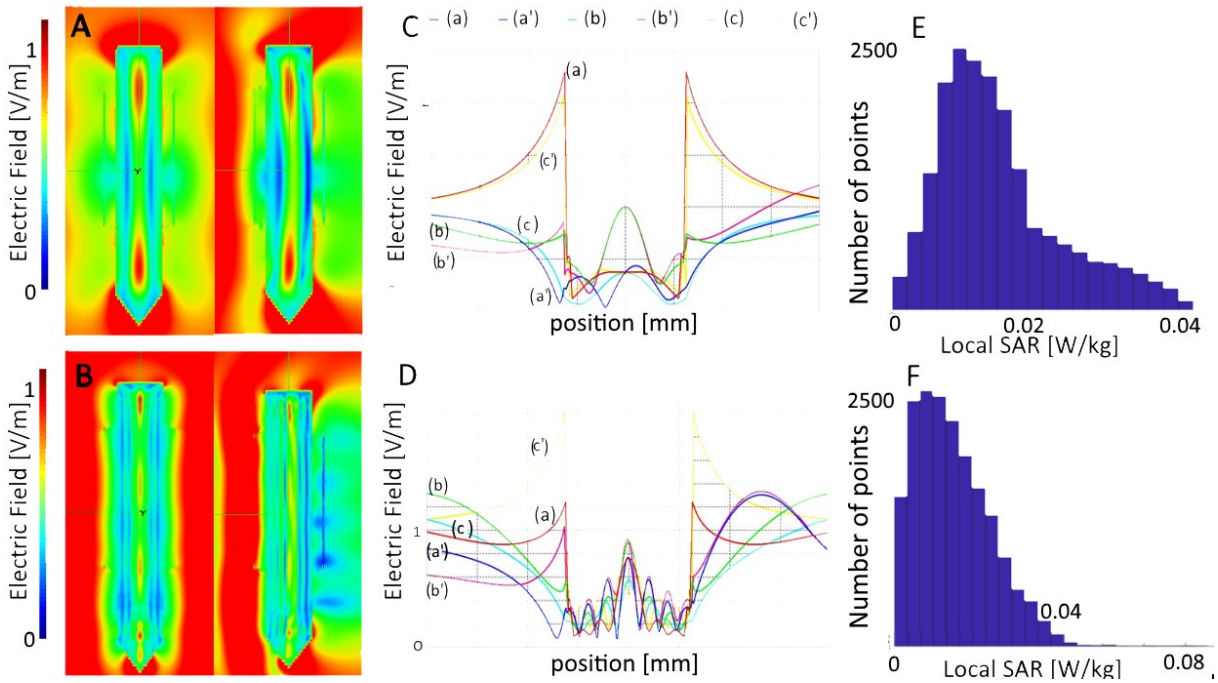

Fig.6

Comment citer ce document :
Bertrand, E., Pasquier, C., Duchez, Girard, Pons, Bonnet, Creuly, Dussap (2018).
High-frequency, high-intensity electromagnetic field effects on Saccharomyces cerevisiae conversion yields and growth rates in a reverberant environment. Bioresource Technology, 260, 264-272. , DOI :
10.1016/j.biortech.2018.03.130

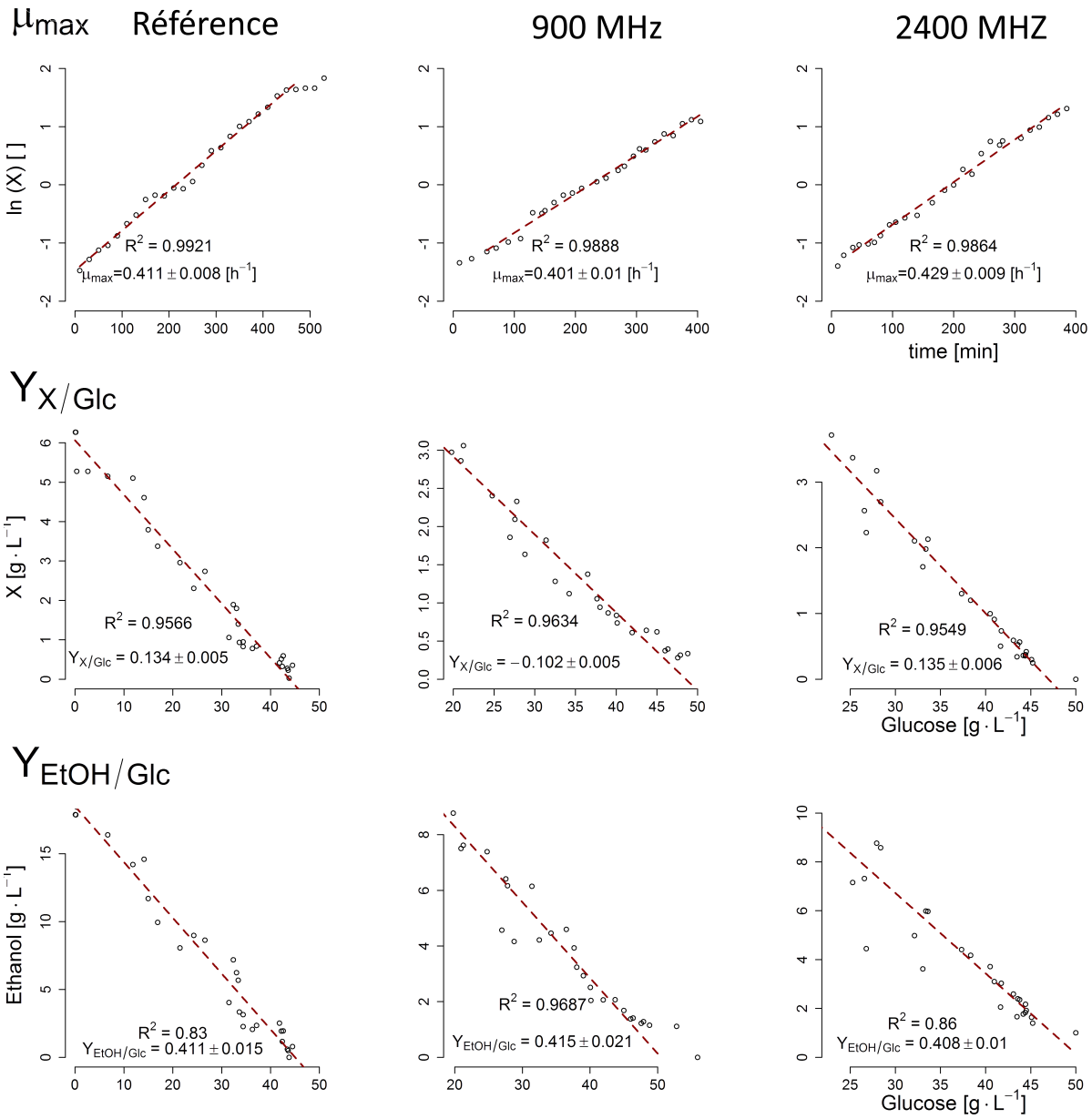

621

622

623 **Table 1.**

	Reference	MSRC 900 MHz	MSRC 2400 MHz
[h^{-1}]	**0.411 ± 0.008**	**0.400 ± 0.010**	**0.429 ± 0.009**
	0.134 ± 0.005	**0.102 ± 0.048**	**0.135 ± 0.006**
	0.411 ± 0.015	**0.415 ± 0.021**	**0.408 ± 0.010**
	0.335 ± 0.011	**0.290 ± 0.012**	**0.305 ± 0.009**
	-0.025 ± 0.001	-0.027 ± 0.002	-0.021 ± 0.003
	0.039 ± 0.003	0.016 ± 0.003	0.018 ± 0.003
	0.0070 ± 0.0006	0.0044 ± 0.0019	0.0045 ± 0.0016
	-0.045 ± 0.002	-0.044 ± 0.001	-0.052 ± 0.0023
	-0.0215 ± 0.0005	-0.0074 ± 0.0001	-0.0073 ± 0.0002
	9-13	**9-13**	**9-13**
[%]	91.9 ± 3.6	94.6 ± 5.1	89.4 ± 2.8
[%]	74.1 ± 7.2	83.9 ± 5.2	105.3 ± 6.2
[$g \cdot L^{-1}$]	0.16 ± 0.1	0.19 ± 0.32	0.5 ± 0.3
Mean Electric Field Inside the Reactor [$V.m^{-1}$]		6.1080	3.4431
Average Local Specific Absorption Rate (SAR) [$W.kg^{-1}$]	-	0.0175	0.0147
Maximum Local Specific Absorption Rate (SAR) [$W.kg^{-1}$]	-	0.0395	0.0794

624 **Figures Legends**

625 **Fig.1:** Schematic representation of the Mode Stirred Reverberation Chamber at Institut Pas-
626 cal.

627

628 **Fig.2: A:** Electric field strength repartition in the MSCR for modes 7/33/14. **B**: MSCR re-
629 sponse at 900 MHz. The red circles represent the bandwidth. **C:** All modes activated in the
630 MSCR for a 900 MHz excitation. **D:** All modes activated in the MSCR for a 2400 MHz excit-
631 ation. **E:** Electric field around the reactor at 900 MHz **F:** Electric field around the reactor at
632 2400 MHz. The reactor is represented in grey at the center of figures E and F.

Fig.3: Measured relative-permittivity (black lines) and electric conductivity (red lines) of the minimal medium before (full line) and after (dotted line) the culture of *Saccharomyces cerevisiae* as a function of the frequency. The periodical oscillations are due to the measurement system.

Fig.4: A: Profiles comparisons for the simulated electric field inside the secondary reactor illuminated with a planar wave at 900 MHz (top left) and 2400 MHz (bottom left). Numbers correspond to the cutting plans presented in figure 1B. **B:** Evaluation of the influence of the electromagnetic field probe (and its protection) insertion into the irradiated part of the reactor on the experimental measurements at 900 MHz. (a) simulated electric field inside the empty reactor; (b) simulated electric field inside the culture medium; (c) simulated electric field after the insertion of the protection for the probe; (d) simulated electric field after the insertion of the probe itself; * represents the value experimentally measured by the probe at the center of the secondary reactor.

Fig.5 A: Free space **s**imulated electric field near the bioreactor at 900 MHz and **B:** 2400 MHz. Barographs are voluntarily limited to 0-1 V/m for a better visualization. **C:** Maximum electric field profile inside the bioreactor for the three-different incident polarizations for (XZ): a, b and c and (YZ): a', b', c' plane at 900 MHz and **D:** 2400 MHz (bottom). **E:** Distribution of the 20000-calculated local SAR inside the bioreactor at 900 MHz and **F:** 2400 MHz.

Fig.6: Determinations of the maximal growth rate (μ_{max}), of the biomass to glucose reaction yield ($Y_{X\text{-}Glc}$), and of the ethanol to glucose reaction yield ($Y_{EtOH\text{-}Glc}$), using linear regressions assuming the Monod hypothesis.

Table Legends

Table 1: Maximal growth rate (μ_{max}) and its standard deviation, Reaction Mass Yields ($Y_{X\text{-}Glc}$: biomass to glucose, $Y_{EtOH\text{-}Clc}$: Ethanol to glucose, $Y_{Am\text{-}Glc}$: Ammonium to glucose, $Y_{AA\text{-}Glc}$: Amino acids to glucose, $Y_{Gly\text{-}Glc}$: Glycerol to glucose, $Y_{Ace\text{-}Glc}$: Acetate to glucose), Respiratory Quotient (RQ mol CO_2/mol O_2), Carbon and Nitrogen Mass Balances (B_C and B_N: percentage of elements recovery considering the products concentration experimental assessment), half velocity constant (K_s : Monod model), Mean electric field inside the reactor, average and maximum Local Specific Absorption Rate (Local SAR) for the selected bioreactor cultures.